Dalton Transactions

Synthesis of First Row Transition Metal Selenomaltol Complexes

Journal:	*Dalton Transactions*
Manuscript ID	DT-ART-03-2018-001170.R1
Article Type:	Paper
Date Submitted by the Author:	14-Jun-2018
Complete List of Authors:	Spiegel, Michael; Baylor University, Chemistry Hoogerbrugge, Amanda; Baylor University, Chemistry and Biochemistry; Baylor University, Chemistry and Biochemistry Truksa, Shamus; Baylor University, Chemistry and Biochemistry Smith, Andrew; Baylor University, Chemistry and Biochemistry Shuford, Kevin; Baylor University, Chemistry and Biochemistry Klausmeyer, Kevin; Baylor University, Chemistry and Biochemistry Farmer, Patrick; Baylor University, Department of Chemistry and Biochemistry

Dalton Transactions

Paper

Synthesis of First Row Transition Metal Selenomaltol Complexes

Michael T. Spiegel, Amanda Hoogerbrugge, Shamus Truksa, Andrew G. Smith, Kevin L. Shuford, Kevin K. Klausmeyer and Patrick J. Farmer*.

Received 00th January 20xx,
Accepted 00th January 20xx
DOI: 10.1039/x0xx00000x

www.rsc.org/dalton

We report an efficent, one-step synthesis of the chelator 3-hydroxy-2-methyl-4-selenopyrone (selenomaltol). Complexes of selenomaltol with Fe(III), Ni(II), Cu(II) and Zn(II) have been prepared and studied by NMR, X-ray crystallography, cyclic voltammetry, EPR and electronic absorption. The Ni(II) and Cu(II) complexes show chemically reversible oxidations which are suggested to be ligand-based. Nuclear independent chemical shifts (NICS) analysis is used to compare aromaticity of the heterocyclic rings of selenomaltol and its chelates. The compounds described here should significantly expand the scope and utility of unusual O,Se-donor chelates.

Introduction

Maltol, 3-hydroxy-2-methyl-4-pyrone (Hma), is a natural product commonly used as a food additive and useful bidentate metal chelator.[1] Maltol complexes have been investigated for use in areas such as cell-labelling,[2] dental care,[3] radiopharmaceuticals,[4] insulin mimetics,[5-7] and enzymatic browning prevention.[8] Over the past two decades, hetero-substituted maltols and their metal complexes have been studied for applications like antimicrobials,[9, 10] metalloprotein inhibition,[10-12] anti-melanoma properties[13] and chelation therapy.[14] Previously our group has reported on the synthesis of the ligands 3-hydroxy-2-methyl-4-pyrone (thiomaltol or Htma) and 3-hydroxy-2-methyl-4-pyrone (dithiomaltol or Httma) and their metal complexes.[13, 15, 16]

A new addition to this family of chelates is selenomaltol, 3-hydroxy-2-methyl-4-selenone (Hsma), first reported in 2008.[17] Despite the wide range of interest in the metal complexes of maltol and its hetero-substitutions, no metal complexes of selenomaltol have yet to be reported. However, the ligand and its aromaticity has been studied by the Tejchman group, who suggested that the chelatoaromatic effect would occur in metal complexes of selenomaltol but be less profound than those of maltol or thiomaltol.[18, 19] We have developed a rapid, high- yield microwave synthesis of selenomaltol, which was used to generate the first homoleptic first row transition metal complexes of selenomaltol. These new complexes have been characterized by X-ray crystallography, electronic absorption, NMR, EPR and cyclic voltammetry. To assess the compounds aromaticity after metal chelation computations of Nuclear Independent Chemical Shifts (NICS) were also done. These mixed O,Se chelating ligands are expected to find utility In a variety of bioinorganic applications such as heavy metal waste remediation.[19]

Scheme 1 Synthesis of selenomaltol from maltol

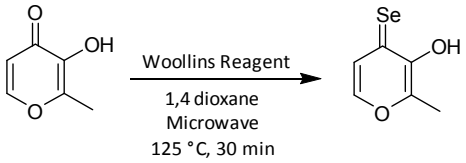

Scheme 2 Synthesis of metal complexes

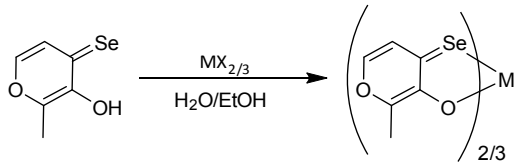

X = $C_2H_3O_2^-$, NO_3^-

M = Zn^{2+}, Cu^{2+}, Ni^{2+}, Fe^{3+}

Results and discussion

Improved Synthesis of Hsma.

The previously reported synthesis of selenomaltol was via reaction of maltol with P_4Se_{10} generated *in situ* from elemental Se and red phosphorus;[17] The reaction took twelve hours to complete and required recrystallization in xylenes. Here we report a modified synthesis, in which maltol is treated directly with Woollins reagent, Scheme 1, and heated to 100°C in a microwave reactor for thirty minutes. Extraction with hexanes and evaporation yields pure selenomaltol, (Hsma) as a red powder in 60% yield. Subsequently, crystals were grown from hexanes as confirmation.

[a] *Department of Chemistry and Biochemistry, Baylor University, Waco, Texas 76798, USA. E-mail Patrick_Farmer@baylor.edu*

Electronic Supplementary Information (ESI) available: Including crystallographic data for Hsma and its metal complexes, synthesis for various thiomaltol species, and EPR details on $Cu(tma)_2$. See DOI: 10.1039/x0xx00000x

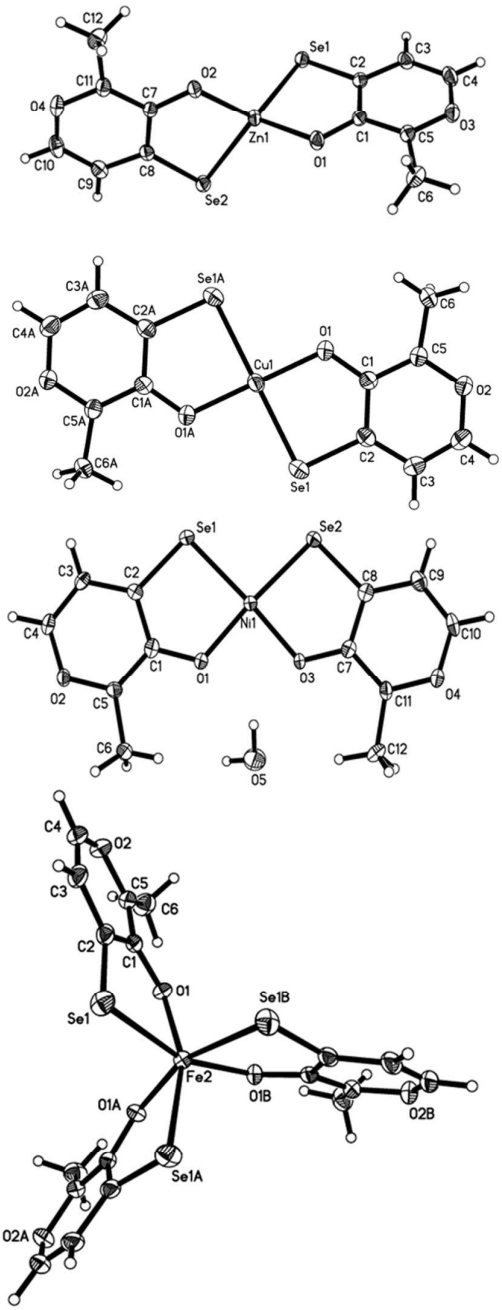

Figure 1 Crystal structures of $Zn(sma)_2$ (**1**), $Cu(sma)_2$ (**2**), $Ni(sma)_2$ (**3**) and $Fe(sma)_3$ (**4**) from top to bottom.

Syntheses and structures of metal complexes

Hsma was then reacted with a series of late first row transition metal ions to generate homoleptic complexes, **Scheme 2.** In a typical synthesis, a slight excess of Hsma in EtOH was added dropwise to an aqueous solution of the desired metal ion, resulting in precipitation. The precipitate was washed with water and hexane and dried via vacuum overnight to give the products $Zn(sma)_2$ (**1**), $Cu(sma)_2$ (**2**), $Ni(sma)_2$ (**3**) and $Fe(sma)_3$ (**4**). Single crystals of each complex were obtained by vapor diffusion of diethyl ether into CH_2Cl_2, and their structures were determined via X-Ray diffractometry, and are shown in **Figure 1**.

The Zn(II) complex **1** has a distorted 4-coordinate tetrahedral geometry. Bond lengths are 1.97 and 2.43 Å for the Zn-O and Zn-Se bonds with a O1-Zn-O3 angle of 120.0° and Se1-Zn-Se2 angle of 125.6°, almost identical to the analogous thiomaltol complex.[20] The Cu(II) complex **2** is 4-coordinate with a *trans* square planar geometry, analogous to the previously published $Cu(tma)_2$ complex.[22] The bond lengths are 1.91 and 2.40 Å for the Cu-O and Cu-Se bonds, respectively. The O1-Cu-Se1 bond angle within the ligand was 88.74°. The Ni(II) complex **3** is also a four coordinate, square planar geometry, but in a *cis* configuration. The average Ni-O and Ni-Se bond distances are 1.88 and 2.28 Å, respectively. There is a slight distortion in the square planar conformation due to its *cis* geometry, with the Se1-Ni-Se2 bond angle 93.86° and the O1-Ni-O3 angle 85.81°. This distortion is slightly more pronounced then that the analogous thiomaltol and maltol Ni complexes.[21] Likewise, the Fe(III) complex **4** has an octahedral *fac* geometry analogous to the previously reported $Fe(tma)_3$.[21] The average Fe-O and Fe-Se bond lengths are 1.99 and 2.61 Å, respectively. The twist angle of the complex of 47.91° is slightly less than that reported for both the Fe maltol and thiomaltol complexes.

EPR characterizations

The oxidation states of complexes **2** and **4** were investigated by electron paramagnetic resonance (EPR), which allows comparisons of ligand field strength and electronic structural variations in transition metal ion complexes. As shown in **Figure 2**, the EPR spectrum of complex 2 displays the axial absorbance expected for square planar d^9 Cu(II) species. The analogous $Cu(tma)_2$ EPR shows $g_{\parallel} = 2.15$ and $g_{\perp} = 2.07$, implying that Hsma is the weaker field ligand (**ESI**). The spectrum of complex 4 is characteristic of a d^5 S = 3/2 system similar to the previously published $Fe(tma)_3$ complex, which also has an octahedral *fac* geometry.[22]

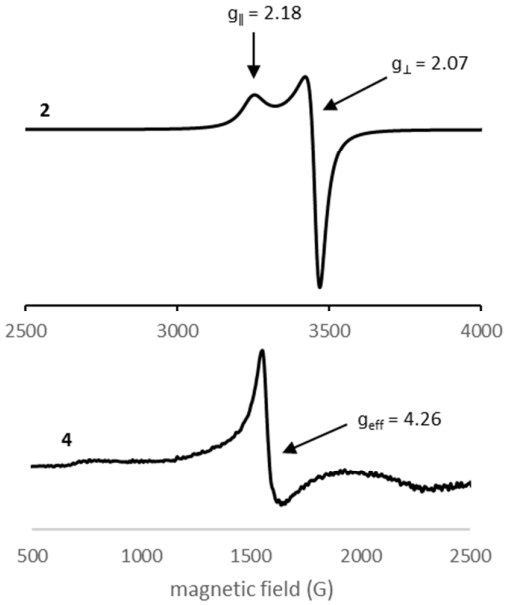

Figure 2 EPR spectra of crystalline powder sample of **2** taken at room temperature (top), and a frozen solution of **4** in toluene at 77 K (bottom).

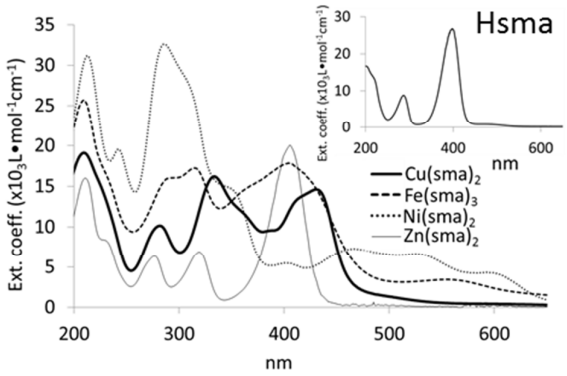

Figure 3 Comparison of normalized absorption spectra of $Zn(sma)_2$ (**1**, line), $Cu(sma)_2$ (**2**, bold), $Ni(sma)_2$ (**3**, dotted), and $Fe(sma)_3$ (**4**, dashed) using the calculated molar extinction coefficient (L $mol^{-1}cm^{-1}$) in CH_2Cl_2. Inset: the absorbance of Hsma over the same range.

Absorption spectra

Electronic absorption spectra for Hsma and its metal complexes are shown in **Figure 3**. Selenomaltol itself has absorbance bands at 287 and 399 nm, the latter resulting in selenomaltol's bright red color. $Zn(sma)_2$ and $Cu(sma)_2$, complexes **1** and **2**, do not share the same low energy transitions (> 500 nm) of $Ni(sma)_2$ and $Fe(sma)_3$, complexes **3** and **4**. These low energy transitions are attributed to ligand/metal charge transfer. In general, the absorption bands for these species are ca. 50 nm lower in energy than those of the analogous thiomaltol complexes,[20, 21] consistent with selenomaltolato being a slightly weaker field donor than thiomaltolato.

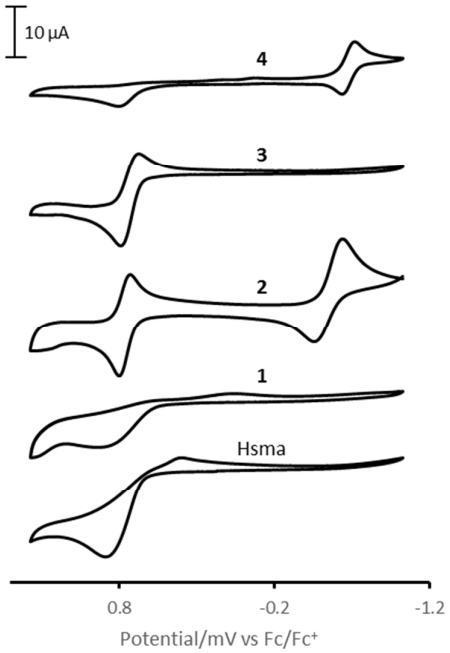

Figure 4 Cyclic voltammograms of Hsma and complexes **1**- **4** in anhydrous CH_2Cl_2 with 0.1 M $TBAPF_6$ as the supporting electrolyte on Pt disc electrode, scan rate 100 mV/s.

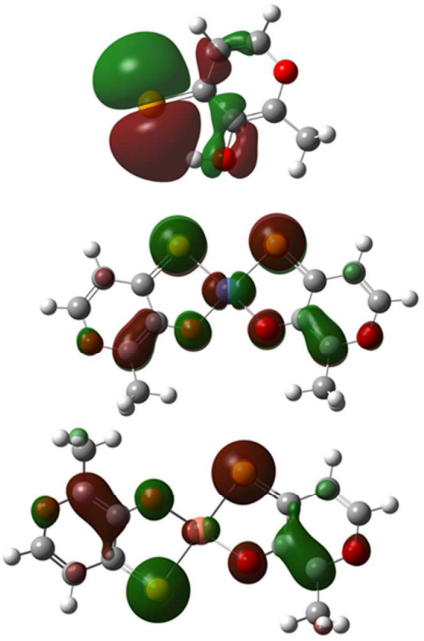

Figure 5 HOMO occupancies of Hsma (top) and $Ni(sma)_2$, (**3**, middle)**,** and the alpha SOMO occupancy of $Cu(sma)_2$, (**2,** bottom).

Cyclic voltammetry

Redox properties of Hsma, **1**, **2**, **3** and **4** were assessed by voltammetry in anhydrous, anaerobic CH_2Cl_2 with 100 mM TBAHFP as an electrolyte. As seen in **Figure 4,** Hsma undergoes irreversible oxidation ca. 0.8 V.

All complexes **1-4** have similar oxidations at close to the same potentials, which suggests that all are attributable to the oxidation of ligand. Indeed, DFT calculations of free Hsma and diamagnetic complexes **1** and **3** suggest that the Se lone pair are dominant in the HOMO of these complexes, **Figure 5**.

Significantly, both the Cu(II) and Ni(II) complexes, **2** and **3,** show chemically reversible oxidations at 0.76 V (ΔE_p = 69 mV, i_{pa}/I_{pc} of .735) and 0.74 V with (ΔE_p = 86 mV, i_{pa}/I_{pc} of 0.748), respectively. The free ligand and the Zn(II) and Fe(III) complexes **1** and **4** display irreversible oxidations at very similar potentials, which suggests that all have significant Se character as above. For complexes **2** and **3**, these oxidations are much more reversible than those reported previously for the analogous thiomaltol complexes (**ESI**), which may suggest significant M-Se delocalization.

Additionally, the Cu(II) and Fe(III) complexes **2** and **4** undergo observable reductions. Complex **2** undergoes a quasi-reversible reduction at -0.51 V (ΔE_p = 105 mV, i_{pa}/I_{pc} .569) which we attribute to $Cu^{II/I}$ couple; the large peak separation is characteristic of the expected reorganization from square planar Cu(II) to tetrahedral Cu(I).[23, 24] Complex **4** undergoes a reversible reduction at -0.68 V (ΔE_p = 59 mV, i_{pa}/I_{pc} .542), which we attribute to the $Fe^{III/II}$ couple; this reduction potential is somewhat more positive than those reported for Fe thiomaltol and maltol complexes.[21] Thus the softer selenone chelate stabilizes the reduced state relative to thione or ketone chelates.

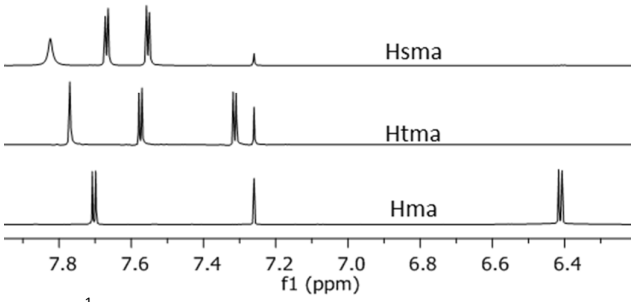

Figure 6 ^{1}H NMR spectra in CD_3Cl of the aromatic region of Hsma, Htma, and Hma from top to bottom.

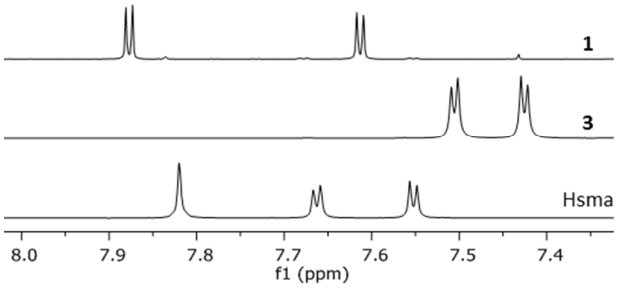

Figure 7 ^{1}H NMR spectra in CD_3Cl in the aromatic region of complex **1**, **3** and Hsma.

NMR characterizations

In previous studies of thio- and dithiomaltol complexes, the downfield shift of the vinylic protons in ^{1}H NMR spectra was interpreted as indicative of aromaticity of the heterocycle, and found to be enhanced by chelation to metal ions.[15,16] The apparent increase in aromaticity was attributed to the stability of the aromatic resonance structure when the ligand was bound to a metal, **Scheme 3**, which was also suggested to engender unique redox and photochemistry. In selenomaltol, we believe the aromatic resonance form is stabilized due to the poor π bond between selenium and carbon.[25] These changes should cause a change in the NMR and bond lengths of these complexes

Scheme 3 Resonance structures related to aromaticity

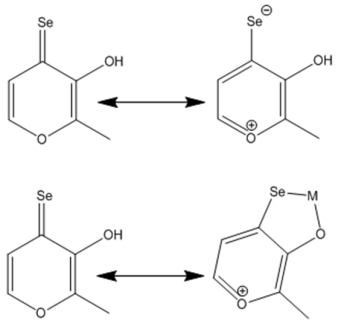

As seen in **Figure 5**, Hsma appears to be slightly more aromatic than thiomaltol.[13-15, 20, 21] However, spectra of complexes **1** and **3** exhibit opposite shifts of the vinylic protons in comparison to the free ligand, with **1** shifting downfield and **3** upfield, as seen in **Figure 6**. These effects are also observed for the analogous thiomaltol complexes.[20, 21]

But a contrary trend is seen in the ^{13}C NMR spectra of Hsma and complexes **3** and **1**, **Figure 7**. Specifically, the unique selenone signal moves from 186 ppm for Hsma to 172 and 175 ppm respectively for complexes **1** and **3**, consistent with greater shielding from the aromatic tautomer. Because of the discrepancy between the ^{13}C and ^{1}H NMR, ^{77}Se NMR was performed to directly probe the increase in electron density on the selenium, **Figure 8**. The ^{77}Se peak of the free ligand is considerably shifted more upfield than one would expect of a selenone (~700 ppm vs. 2000 ppm), closer to that of a selenoamide.[26]

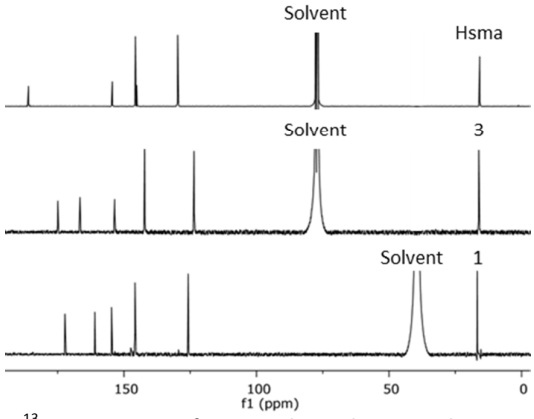

Figure 8. ^{13}C NMR spectra of Hsma and complexes **3** and **1**.

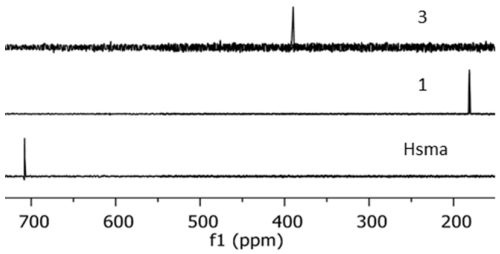

Figure 9 ^{77}Se NMR spectra in CD_3Cl of complex **1**, **3** and Hsma.

When complexed, the ^{77}Se peak is shifted farther upfield, suggesting more electron-density on the selenium, as in the zwitterionic aromatic resonance structure shown in **Scheme 3**. The greater ^{77}Se peak shift in complex **1** vs complex **3** is likely due to the Zn^{2+} ion being better electron donor than the Ni^{2+} ion. Thus, there is good agreement between the ^{77}Se and ^{13}C NMR spectral analysis, which counters that of the ^{1}H NMR, regarding the resonance structures of metal complexed ligands.

Other measures of aromaticity

To further characterize the pseudo-aromaticity of zwitterionic resonance form and its enhancement when complexed to a metal ion, several other approaches were investigated. Crystallographic data relating to alteration of double and single bonds within a heterocyclic ring can be used to distinguish delocalization and aromaticity.[27] Bond distances for C-Se and various C-C bonds within the ring system are shown in **Table 1**.

Table 1 Select bond distances of Hsma and complexes **1**-**4**.

	C2-Se1 Å	C1-C2 Å	C2-C3 Å	C3=C4 Å	C1=C5 Å
Hsma	1.827(2)	1.421(3)	1.420(3)	1.344(3)	1.358(3)
$Zn(sma)_2$ **(1)**	1.866(2)	1.425(3)	1.414(3)	1.348(3)	1.392(3)
$Cu(sma)_2$ **(2)**	1.854(2)	1.416(3)	1.411(3)	1.348(3)	1.386(4)
$Ni(sma)_2$ **(3)**	1.869(4)	1.408(5)	1.400(5)	1.354(5)	1.389(5)
$Fe(sma)_3$ **(4)**	1.855(3)	1.426(4)	1.407(4)	1.344(5)	1.386(4)

As previously mentioned, the C-Se bond distances in **Table 1** are longer than that expected for a C=Se double bond, especially when complexed to a metal ion.[17, 28] Likewise, the ring C=C double bonds are longer and the single bonds shorter when complexed, suggesting enhanced aromaticity in the complexed heterocycles.

A similar examination of the M-Se bonds also implies the dominance of the zwitterionic resonance state shown in **Scheme 3**. **Table 2** compares the predicted ion bond lengths for metal-selenium bonds with the Se in the neutral and anionic form. As seen, the observed bond lengths are best matched by its reduced ionic radius, as would be seen for the zwitterion. Also note that the Fe(III) complex **4** displays the longest M-Se and M-O bonds, likely due to its high spin state.

Table 2 Predicted and observed M-Se bond lengths

complex	M- Se^0 Å [(a)]	M-Se^{2-} Å [(a)]	Observed Å
$Fe(sma)_3$ **(4)**	1.945	2.765	2.6114(6)
$Ni(sma)_2$ **(3)**	1.790	2.610	2.2799(6)
$Cu(sma)_2$ **(2)**	1.870	2.690	2.4002(2)
$Zn(sma)_2$ **(1)**	1.900	2.720	2.4246(3)

(a) sum of ionic radii for metal ion and Se^O or Se^{2-}.[29, 30]

A computational measure of aromaticity is by nuclear independent chemical shifts (NICS) analysis, based on the predicted magnetic shielding due to the aromatic ring current. The magnetic shielding can be calculated in the centre of the ring, which is determined by the non-weighted mean of the heavy atom coordinates ($NICS(0)_{iso}$) or at 1 Å above it ($NICS(1)_{zz}$). Strongly negative NICS values are indicative of high aromaticity.[31, 32]

Table 3 Nuclear independent chemical shifts (NICS)

complex	$NICS(0)_{iso}$	$NICS(1)_{zz}$
Hsma/Htma/Hma	-1.85/-1.65/-1.50	-8.96/-9.00/-5.77
$Zn(sma)_2/(tma)_2$	-3.41/-3.53	-12.95/-13.09
$Cu(sma)_2/(tma)_2$	-2.57/-3.42	-10.37/-12.27
$Ni(sma)_2/(tma)_2$	-4.22/-4.67	-14.12/-14.44
$Fe(sma)_3/(tma)_3$	-3.87/-4.04	-15.91/-16.43

Both $NICS(0)_{iso}$ and $NICS(1)_{zz}$ analysis were performed on free ligands Hsma, Htma, and Hma as well as on the Zn(II), Ni(II) and Fe(III) thio- and selenomaltolato complexes, **Table 3**. Of the free ligands, selenomaltol has a greatest degree of aromaticity for the $NICS(0)_{iso}$ measurement, but thiomaltol in the $NICS(1)_{zz}$ assessment. Likewise, the Ni(II) complexes have the greatest degree of aromaticity by $NICS(0)_{iso}$, while the Fe(III) complexes the most aromatic by $NICS(1)_{zz}$ assessments. Overall, there is a significant increase in aromaticity for the metal complexes when compared to the free ligands, for both the thio- and selenomaltolato species.

Conclusions

A new high-yield synthesis of selenomaltol is described. The crystal structures of the homoleptic Zn(II), Cu(II), Ni(II) and Fe(III) complexes have been determined, which are the first reported for this unique chelator. The complexes exhibit analogous coordination geometries to previously reported thiomaltol complexes. Electrochemical properties found an unexpected reversible oxidation in the Ni and Cu species attributed to the ligand, which are subjects of ongoing research. Additionally, selenomaltol is being assessed as a heavy metal chelator for potential medical applications.

Experimental

Materials

Maltol, $Fe(NO_3)_3 \bullet 9\ H_2O$, $Zn(C_2H_3O_2)_2$, and $Ni(C_2H_3O_2)_2 \bullet 4\ H_2O$ were purchased from Alfa Aesar and used as received. All solvents used, Woollins reagent, Lawessons reagent and Tetrabutylammonium Hexafluorophosphate (TBAPF6) were purchased from Sigma-Aldrich. The thiomaltol ligand was prepared in a similar fashion to selenomaltol and its metal complexes were prepared using methods similar to previously published complexes (**ESI**).[15,22]

Physical measurements

Electronic absorption spectra were recorded with an Agilent 8453 diode array spectrophotometer. Microwave syntheses were carried out in an discover SP microwave system. Mass spectra were obtained on a Thermo Electron Linear Trap Quadrupole Orbitrap Discovery mass spectrometer. NMR spectra were recorded on a 600 Hz NMR system. EPR characterizations were recorded from solid polycrystalline samples of **2** and $Cu(tma)_2$ and complex **4** at 77 K with an EMXplus EPR spectrometer. Conditions for **2**: microwave frequency 9.86 GHz, microwave power 2.00 mW, modulation amplitude 4.00 G, time constant 0.01 ms, sweep width 2000 G, sweep time 20.0 ms. Conditions for **4**: microwave frequency 9.47 GHz, microwave power 2.00 mW, modulation amplitude 4.00 G, time constant 0.01 ms, sweep width 6000 G, sweep time 20.0 ms.

Cyclic voltammetry experiments were performed using a CHI-760B potentiostat in dry-degassed CH_2Cl_2 with 0.1 M tetrabutylammonium hexafluorophosphate ($TBAPF_6$) as the supporting electrolyte. The cells consisted of a platinum working electrode (3.0 mm dia.), AgCl/Ag reference, and a coiled Pt auxiliary electrode. Measured potentials were corrected using a ferrocene standard, with Fe/Fe^+ couples set to 229 mV vs. NHE.

Crystallographic data was collected on crystals with dimensions 0.198 x 0.184 x 0.125 mm^3 for $Fe(sma)_3$, 0.136 x 0.089 x 0.020 mm^3 for $Ni(sma)_2$, 0.242 x 0.113 x 0.083 mm^3 for $Cu(sma)_2$ and 0.404 x 0.141 x 0.101 mm^3 for $Zn(sma)_2$. Data was collected at 110 K on a Bruker D8 quest using Mo-K (λ = .71073 Å) radiation. The data was processed using the Bruker AXS SHELXTL software, version 6.10. Crystallographic parameters for structural determinations of selenomaltol, $Fe(sma)_3$, $Ni(sma)_2$, $Cu(sma)_2$ and $Zn(sma)_2$ are given in the **ESI.**

Computational Details

All calculations were done at the B3LYP/6-311+G(d,p) computational level using Gaussian09.[31] For the NICS calculations, the GIAO method was used to calculate the magnetic shielding tensor of a ghost atom. Due to the systems being symmetrical, the NICS values for only one of the rings are shown. Firstly, the ring is aligned along the x and y-axes so the face of the ring is in the z-direction. Next, a ghost atom is placed in the center of the ring either within the same plane (NICS(0)iso) or 1.0 Å above the ring (NICS(1)zz). A property of ghost atoms is that they will not interact with other atoms, so the NICS(0)iso and NICS(1)zz can be measured simultaneously. The NICS(0)iso represents the negative of isotropic shielding tensor, while the NICS(1)zz represents the negative of the tensor in the zz direction. All NICS values are in ppm.

Synthesis of selenomaltol (Hsma)

Selenomaltol was prepared by dissolving 0.4192 grams (3.324 mmol) of maltol in 15 mL of anhydrous 1,4-dioxane in a 35 mL microwave reaction vessel. Woollins reagent (0.5650 g, 1.062 mmol) was added to the vessel, and the mixture heated in the microwave for 30 minutes at 125 °C. Water was added to the resulting black mixture. Extraction with hexane produced a dark red organic phase, which yielded pure selenomaltol after hexane was removed via rotavap. The resulting red powder was washed with cold water and stored as a solid. The compound was crystallized via slow evaporation of hexanes top produce samples suitable for X-ray diffraction. Yield 0.3771 grams (60%). ESI MS: m/z (pos.) 190.9604 (M +H) ^{1}H NMR (600 MHz, $CDCl_3$): δ 7.68 (d,1H), 7.55 (d,1H), 2.30 (s, 3H), δ 7.83 (s, 1H). ^{13}C NMR (600 MHz, $CDCl_3$): δ 186, 154, 146, 145, 130, 16.

Synthesis of Zn(sma)$_2$ (1)

A sample of Hsma (0.0610 g, 0.3194 mmol) was dissolved in 2 mL of ethanol to form a bright red solution. $Zn(C_2H_3O_2)_2$ (0.0293 g, 0.1597 mmol) was then dissolved in 3 ml of DI water and stirred under nitrogen. The selenomaltol mixture was added drop wise to the zinc solution, immediately forming a yellow precipitate. The solution was centrifuged and the pellet washed with hexane twice to remove any excess selenomaltol. The flask was placed under vacuum to dry overnight and yielded 0.0467 g (79%) of an orange solid. The compound was crystallized in CH_2Cl_2 by vapor diffusion with hexane to produce samples suitable for X-ray diffraction. ^{1}H NMR (600 MHz, $CDCl_3$): δ 7.87 (d,1H), 7.62(d,1H), 2.56 (s, 3H). ^{13}C NMR (600 MHz, $(CD_3)_2SO$): δ 172, 161, 155, 146, 126, 17. ESI MS: m/z (pos.) 442.8263(M +H).

Synthesis of Cu(sma)$_2$ (2)

A sample of Hsma (0.0627 g, .3316 mmol) was dissolved in 2 mL of ethanol. $Cu(OAc)_2$ (0.0300 g, .1652 mmol) was then dissolved in 3 mL of DI water and stirred under nitrogen. The selenomaltol mixture was added drop wise to the copper solution, immediately forming a brown precipitate. An additional 10 ml of water was added to further facilitate precipitation. The resulting mixture was filtered and washed with 5 ml of hexanes twice and an additional 5 ml of DI water. The solid was placed under vacuum to dry overnight and yielded 0.0511 g (70%) of a reddish-brown solid. The compound was crystallized in CH_2Cl_2 by vapor diffusion with diethyl ether to produce samples suitable for X-ray diffraction. ESI-MS: m/z (pos.) 441.8281 (M+H).

Synthesis of Ni(sma)$_2$ (3)

A sample of Hsma (0.0565 g, 0.2974 mmol) was dissolved in 2 mL of ethanol. $Ni(C_2H_3O_2)_2 \bullet 4\ H_2O$ (0.0367 g, 0.1477 mmol) was dissolved in 3 mL of DI water and stirred under nitrogen. The selenomaltol mixture was added drop wise to the nickel solution, forming a dark purple precipitate. An additional 10 ml of water was added to further facilitate precipitation. The resulting mixture was filtered and washed with 5ml of hexanes twice and an additional 5 ml of DI water. The solid was placed under vacuum to dry overnight and yielded 0.0486 g (79%) of a black solid. The compound was crystallized in CH_2Cl_2 by vapor diffusion with diethyl ether to produce samples suitable for X-ray diffraction. ^{1}H NMR (600 MHz, $CDCl_3$): δ 7.50 (d,1H), 7.42 (d,1H), 2.45 (s, 3H). ^{13}C NMR (600 MHz, $CDCl_3$): δ 175, 167, 154, 142, 124, 16. ESI-MS: m/z (pos.) 436.8341 (M+H).

Synthesis of Fe(sma)$_3$ (4)

A sample of Hsma (0.0631 g, 0.3338 mmol) was dissolved in 2 mL of ethanol. $Fe(NO_3)_3 \bullet 9\ H_2O$ (0.0433 g, 0.1073 mmol) was dissolved in 3 mL of DI water and stirred under nitrogen. The selenomaltol mixture was added drop wise to the iron solution, immediately forming a black precipitate. An additional 10 ml of water was added to further facilitate precipitation. The resulting mixture was filtered and washed with 5ml of hexanes twice and an additional 5 ml of DI water. The solid was placed under vacuum to dry overnight and yielded 0.0561 g (84%) of a black solid. The compound was crystallized in CH_2Cl_2 by vapour diffusion with hexane to produce samples suitable for X-ray diffraction. ESI MS: m/z (pos.) 433.8255 (M+ - sma). Anal. calc'd for $H_{15}C_{18}Se_3O_6Fe$: C, 34.87; H, 2.44. Found: C, 34.95; H, 2.47.

Acknowledgements

This study was supported in part by funds from the Faculty Research Investment Program and the Vice Provost for Research at Baylor University and the Chemical Sciences, Geosciences, and Biosciences Division, Office of Basic Energy Sciences, Office of Science, U. S. Department of Energy under Award Number DE-SC0010212. We also acknowledge departmental support from Baylor University Facilities for Mass Spectroscopy, NMR, EPR and Crystallography. The authors would also like to acknowledge Dr. Murugaeson Kumar for his help on EPR data collection.

References

1. K. H. Thompson, C. A. Barta and C. Orvig, *Chemical Society Reviews*, 2006, **35**, 545-556.
2. B. L. Ellis, A. K. Duhme, R. C. Hider, M. B. Hossain, S. Rizvi and D. van der Helm, *Journal of Medicinal Chemistry*, 1996, **39**, 3659-3670.
3. M. C. Barret, M. F. Mahon, K. C. Molloy, J. W. Steed and P. Wright, *Inorganic Chemistry*, 2001, **40**, 4384-4388.
4. H. Luo, S. J. Rettig and C. Orvig, *Inorganic Chemistry*, 1993, **32**, 4491-4497.
5. S. J. Lord, N. A. Epstein, R. L. Paddock, C. M. Vogels, T. L. Hennigar, M. J. Zaworotko, N. J. Taylor, W. R. Driedzic, T. L. Broderick and S. A. Westcott, *Canadian Journal of Chemistry*, 1999, **77**, 1249-1261.
6. M. Melchior, K. H. Thompson, J. M. Jong, S. J. Rettig, E. Shuter, V. G. Yuen, Y. Zhou, J. H. McNeill and C. Orvig, *Inorganic Chemistry*, 1999, **38**, 2288-2293.

7. B. D. Liboiron, K. H. Thompson, G. R. Hanson, E. Lam, N. Aebischer and C. Orvig, *Journal of the American Chemical Society*, 2005, **127**, 5104-5115.
8. V. Kahn, in *Enzymatic Browning and Its Prevention*, American Chemical Society, 1995, vol. 600, ch. 22, pp. 277-294.
9. M. E. Helsel, E. J. White, S. Z. A. Razvi, B. Alies and K. J. Franz, *Metallomics*, 2017, **9**, 69-81.
10. S. R. Schlesinger, B. Bruner, P. J. Farmer and S.-K. Kim, *Journal of Enzyme Inhibition and Medicinal Chemistry*, 2013, **28**, 137-142.
11. D. P. Martin, P. G. Blachly, A. R. Marts, T. M. Woodruff, C. A. F. de Oliveira, J. A. McCammon, D. L. Tierney and S. M. Cohen, *Journal of the American Chemical Society*, 2014, **136**, 5400-5406.
12. J. A. Jacobsen, J. L. Fullagar, M. T. Miller and S. M. Cohen, *Journal of Medicinal Chemistry*, 2011, **54**, 591-602.
13. D. Brayton, F. E. Jacobsen, S. M. Cohen and P. J. Farmer, *Chemical Communications*, 2006, DOI: 10.1039/B511966A, 206-208.
14. J. A. Lewis and S. M. Cohen, *Inorganic Chemistry*, 2004, **43**, 6534-6536.
15. M. Backlund, J. Ziller and P. J. Farmer, *Inorganic Chemistry*, 2008, **47**, 2864-2870.
16. B. Bruner, M. B. Walker, M. M. Ghimire, D. Zhang, M. Selke, K. K. Klausmeyer, M. A. Omary and P. J. Farmer, *Dalton Transactions*, 2014, **43**, 11548-11556.
17. W. Tejchman, K. Zborowski, W. Lasocha and L. M. Proniewicz, *Heterocycles*, 2008, **75**, 1931-1942.
18. W. Tejchman, E. Żesławska, K. Zborowski, W. Nitek and M. Żylewski, *ARKIVOC*, 2015, DOI: http://dx.doi.org/10.3998/ark.5550190.p009.262, 216-230.
19. W. Tejchman, L. M. Proniewicz and K. K. Zborowski, *Journal of Physical Organic Chemistry*, 2015, **28**, 536-541.
20. J. A. Lewis, B. L. Tran, D. T. Puerta, E. M. Rumberger, D. N. Hendrickson and S. M. Cohen, *Dalton Transactions*, 2005, DOI: 10.1039/B505034K, 2588-2596.
21. J. A. Lewis, D. T. Puerta and S. M. Cohen, *Inorganic Chemistry*, 2003, **42**, 7455-7459.
22. E. Orlowska, A. Roller, M. Pignitter, F. Jirsa, R. Krachler, W. Kandioller and B. K. Keppler, *Science of The Total Environment*, 2017, **577**, 94-104.
23. A. M. Bond and R. L. Martin, *Coordination Chemistry Reviews*, 1984, **54**, 23-98.
24. J. P. Barbier, A. El Biyyadh, C. Kappenstein, N. D. Mabiala and R. P. Hugel, *Inorganic Chemistry*, 1985, **24**, 3615-3620.
25. H. J. Reich and R. J. Hondal, *ACS Chemical Biology*, 2016, **11**, 821-841.
26. E. R. Cullen, F. S. Guziec, C. J. Murphy, T. C. Wong and K. K. Andersen, *Journal of the American Chemical Society*, 1981, **103**, 7055-7057.
27. T. M. Krygowski, H. Szatylowicz, O. A. Stasyuk, J. Dominikowska and M. Palusiak, *Chemical Reviews*, 2014, **114**, 6383-6422.
28. T. W. Keal and D. J. Tozer *, *Molecular Physics*, 2005, **103**, 1007-1011.
29. R. D. Shannon, *Acta Crystallographica Section A*, 1976, **32**, 751-767.
30. J. C. Slater, *The Journal of Chemical Physics*, 1964, **41**, 3199-3204.
31. M. J. Frisch, G. W. Trucks, H. B. Schlegel, G. E. Scuseria, M. A. Robb, J. R. Cheeseman, G. Scalmani, V. Barone, B. Mennucci, G. A. Petersson, H. Nakatsuji, M. Caricato, X. Li, H. P. Hratchian, A. F. Izmaylov, J. Bloino, G. Zheng, J. L. Sonnenberg, M. Hada, M. Ehara, K. Toyota, R. Fukuda, J. Hasegawa, M. Ishida, T. Nakajima, Y. Honda, O. Kitao, H. Nakai, T. Vreven, J. A. Montgomery, J. E. Peralta, F. Ogliaro, M. Bearpark, J. J. Heyd, E. Brothers, K. N. Kudin, V. N. Staroverov, R. Kobayashi, J. Normand, K. Raghavachari, A. Rendell, J. C. Burant, S. S. Iyengar, J. Tomasi, M. Cossi, N. Rega, J. M. Millam, M. Klene, J. E. Knox, J. B. Cross, V. Bakken, C. Adamo, J. Jaramillo, R. Gomperts, R. E. Stratmann, O. Yazyev, A. J. Austin, R. Cammi, C. Pomelli, J. W. Ochterski, R. L. Martin, K. Morokuma, V. G. Zakrzewski, G. A. Voth, P. Salvador, J. J. Dannenberg, S. Dapprich, A. D. Daniels, Farkas, J. B. Foresman, J. V. Ortiz, J. Cioslowski and D. J. Fox, *Journal*, 2009, DOI: citeulike-article-id:9096580.
32. Z. Chen, C. S. Wannere, C. Corminboeuf, R. Puchta and P. v. R. Schleyer, *Chemical Reviews*, 2005, **105**, 3842-3888.